Evaluation of Over Current Relay Settings Optimization for Multi-infeed DG-connected-grid

NAEMA M. MANSOUR*, ABDELAZEEM A. ABDELSALAM, EMAD ElDEEN OMRAN, EYAD S. ODA.
Department of Electrical Engineering,
Suez Canal University,
Ismailia,
EGYPT

**Corresponding Author*

Abstract: - Increasing the short-circuit current magnitude and bidirectional flow in a multi-infeed DG-connected grid have significant impacts on protection systems based on over-current relays (OCRs). An adaptive protection scheme based on defining the optimal setting of a directional OCR (DOCR) has recently been introduced as a solution for mis-coordination and false tripping issues associated with DG penetration increase. In this paper, this approach is highlighted, and its performance in different operating modes of the DG-connected grid is evaluated. Genetic algorithm (GA), and gray wolf optimization (GWO) have been used to provide optimized values of the time multiplier setting (TMS) of the DOCR scheme. Different faults at different locations with different DG locations and sizes are studied. The international electrotechnical commission (IEC) micro-grid benchmark and different DG units are modeled with MATLAB Simulink and ETAP software to carry out and test all these operating modes and evaluate this scheme. The ability of this scheme to maintain the coordination between the forward and reverse main and backup relays for each fault location is focused on in this study.

Key-Words: - Distributed generators, Directional over current relay, Genetic Algorithm, Gray Wolf, Time Multiplier Setting; coordination time interval (CTI), Inverse Definite Minimum Time (IDMT)

Received: July 18, 2022. Revised: April 15, 2023. Accepted: May 19, 2023. Published: June 26, 2023.

1 Introduction

Increasing the DG penetration is always accompanied not only by increasing the short-circuit current but also by an obvious change in the relaying fault current either by increasing or decreasing in magnitude or change in direction according to the DG connection point relative to the relaying points. Since the OCR operation is based only on the fault current magnitude measured at the relaying points, the DG connection is strongly affecting its performance and coordination. Any changes in the fault current direction and magnitude at any point within the distribution network would strongly affect the operation and coordination of the relaying scheme. The coordination principle of OCRs depends on the grading of the fault current from the upstream to the downstream points of the radial network. Due to the DG connection to the distribution network, its radial nature has been lost, the challenges concerning short circuit capacity, and protection coordination has been introduced and its impacts on the protection system have been investigated. From these impacts that are highlighted by many works of literature change in the direction of fault current flow, increase or decrease of fault current magnitude measured at the relaying points, the blindness of backup relays when the high-size DG units are connected between the main and backup relays, adjacent feeder mis-trapping for multi-parallel feeders, and the mis-coordination between two or more cascaded pairs of relays depending on the DG size, type, and location relative to the fault point, [1], [3], [4], [5], [6], [7]. Many attempts have been introduced in the literature to mitigate the impacts of DG units on the relaying scheme of the distribution network to which they are connected; some attempts are related to conventional protection strategies, and others are related to modified protection schemes, [8]. Disconnection of DG units, resizing of protective devices, directional protection, fault current limiter, limiting DG size, multiagent-based method, non-slandered characteristics, and the optimal determination of the relay settings to minimize the

overall relay operating time for primary and backup scenarios, all these methods were introduced in the works of literature for DG impacts mitigations on the OCR scheme coordination, [2], [9]. From these suggested solutions, the optimization of the directional OCR settings has been introduced by many researchers recently to overcome the protection coordination problems due to bidirectional fault currents and to provide an adaptive OVR setting, [10], [11], [12], [13], [14], various optimization tools have been introduced in the works of literature to formulating this method. In [10], GA has been used as an optimization tool, and the coordination between every pair of cascaded relays is studied. In [11], Water Cycle Algorithm (WCA), and Particle Swarm Optimization (PSO) are used for comparative analysis, the authors just focused on the main primary and backup relays for each fault location, ignoring the overall backup relays that the reverse fault current is passed through. Adaptive Clonal selection algorithm of the artificial immune system(AIS) is used in, [12], to provide the optimized TMSs, and the novel optimization solvers such as modified PSO, teaching-learning, GWA, moth-flame, and PSO algorithms were used in [13], GA, PSO, and teaching–learning based optimization(TLBO) algorithm were used in, [14].

Other several optimization tools are introduced by the pieces of literature to provide the optimization setting of relay scheme curves such as the Nelder-Mead (NM) simplex search method and (PSO) in, [15], Artificial bees colony (ABC) is employed in, [16], Honey Bee algorithm is used in, [17].

Most of this literature is concerned basically with minimizing the overall operating time of the relaying protection scheme without regard to the performance of all the backup relays by which the fault current was sensed. Reducing the overall computational time by using a modern optimization tool is not the main objective of this study, but the evaluation of the validity of the optimal determination of the relay settings method at different operation modes of DG-connected multi-infeed grid, and different fault scenarios is the objective. The effectiveness of the optimization techniques in the resetting process of the DOCR scheme to cover all the fault scenarios has been highlighted in this paper using GA, and GWA.

In this study, the efficacy of the optimized standard and non-standard curves of directional and non-directional OCR schemes that were introduced by several pieces of literature are tested for different operation modes of DG-connected multi-infeed grids with different fault scenarios and different DG types, locations, and sizes to evaluate their capabilities of mitigating the selectivity problems associated with DG high penetration. To validate the efficacy of the optimized relaying setting, the standard IEC micro-grid structure with DG interfacing is simulated by the MATLAB Simulink package and verified by ETAP software.

The paper is organized as follows. Section II describes the IEC and different DG units that are simulated with MATLAB and ETAP simulators. The problem formulation and DG impacts are summarized in section III. IV. Operating modes and optimized curve settings are briefly described in section III. Optimal settings of non-directional and DOCR are tested in sections V and VI. Non-slandered OCR characteristics and islanding mode operation are discussed in sections VII and VIII. And the study is concluded in section IX.

2 Simulation Model

To test and evaluate the coordination of the relaying scheme, the International Electrotechnical Commission (IEC) micro-grid shown in Fig. 1 is modeled. IEC micro-grid is a 25 kV distribution network connected to the utility of 120 kV, through a 120/25 kV step-down transformer rated at 1000 MVA. Six loads with 3.273MVA at the six buses of the network, [18]. Four DG units (DG1to DG4) with different sizes (9 - 9 - 6 - 9MVA), DG1 and DG2 are synchronous generator-based types, DG3, and DG4 are type 4 and DFIG based wind farms respectively are modeled and connected at different locations on the IEC network to investigate the DG impacts, see Appendix for model data. Six-inverse over current relays (R_1-R_6) are set and coordinated for different modes of operation (DG at different locations, islanding mode).

Load flow analysis, fault analysis studies, and the optimization of the TMS values of OCRs are carried out using MATLAB/Simulink package, then the obtained results are tested by using ETAB software, by inserting the obtained values of TMS as an input to the relay parameters settings and carry out the faults at different locations and test the operation of the related relays for each fault location.

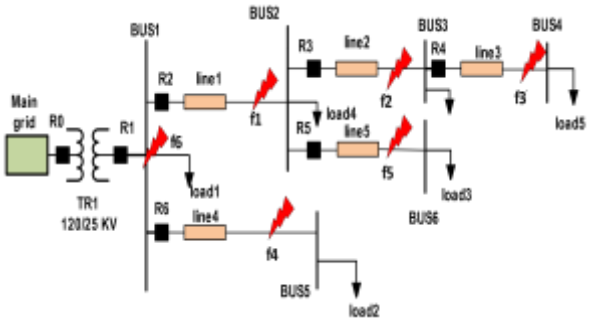

Fig. 1: IEC 6-bus radial network arrangement

3 DG Impacts and Problem Formulation

DG impacts on the distribution network relaying system as concluded in the pieces of literature can be summarized as:

1) Mis-coordination between the cascaded relays.
2) Delaying the backup relays, with DG penetration increase may lead to blinding.
3) Mis-tripping due to the multi-infeed topology and reversing of power flow.
4) Islanding condition.

In addition to DG size, the location of DG units with respect to the relaying point is the main factor for the emergence of one or more of the problems mentioned above as follow: -

1) DG units located at the upstream point of the two primary and backup relays may cause mis-coordination and mis-tripping in the case of high penetration of DG units. Also, if the DG connection point is located upstream of the primary relay and downstream of the backup one, mis-coordination due to delaying of the backup relays or blinding may occur.
2) DG connection point is located at the far end of the feeder or the adjacent feeder, the mis-tripping due to reverse was strongly predicted.

The adaptive protection based on the optimal determination of the directional relay settings for standard and non-standard characteristics (the approach that is relied on the hypothesis that the loss of the relay's selectivity if the fault current level is increased behind the value at which the maximum current multiplier setting CMS_{max} is reached) has been introduced as a solution for the mis-coordination problem. A detailed study of this approach will be carried out and verified with ETAP and MATLAB, and GA is used as an optimization tool.

The optimization algorithms are used to provide the optimized values of TMS to restore the relay setting curves selectivity by minimizing the total operating time of the relays, ensuring coordination between the main and backup relays. The OC coordination problem is formulated as an objective function with several constraints related to coordination time between main and backup relays, the minimum operating time of relays, and the minimum values of coordination time interval (CTI). GA is used to achieve the optimal settings for the OC relays by minimizing the relay's total operating time by solving the objective function.

According to the typical IDMT characteristic equation, the operating time is directly proportional to the values of TMS, on the other hand, it is inversely proportional to the value of CMS as in Equation (1).

$$t_{op} = \frac{0.14 * TMS}{(CMS)^{0.02} - 1} \quad (1)$$

Where TMS is the time multiplier setting and CMS is the current multiplier setting of the relay.
Equation (1) could be rearranged as:

$$t_{op} = a * TMS \quad \text{Where} \quad a = \frac{0.14 * TMS}{(CMS)^{0.02} - 1} \quad \text{and}$$

$$CMS = \frac{I_f}{I_{pick\ up} * CTR} \quad (2)$$

Where I_f is denoted as the fault current, CTR is the CT ratio and $I_{pick\ up}$ is the pickup current of the relay. In GA, the objective function (OF) is given by equation (3).

$$min(t_{op}) = \sum_{i=1}^{m} \sum_{f=1}^{n} a_{if}\, TMS_{if} \quad (3)$$

Where m corresponds to the number of relays. While n is the number of fault locations, and t_{if} is the operating time of relay i during a fault at location f.

- For the IEC six-bus network, there are six relays (R_1 to R_6] and five fault locations (F_1 to F_5).
- Six constraints through the bounds of the relay operating time. The minimum operating time of each relay is taken as 0.2 sec. $t_{op(min)} \leq t \leq t_{op(max)}$ where $t_{op(min)}$ is the minimum operating time and $t_{op(\max)}$ the maximum operating time.
- Five constraints through the coordination between the six relays. The CTI is set to its typical value of 0.3 sec. The constraint for the coordination time interval is given by $t_{backup} - t_{primary} \geq 0.3$.

- The constraints related to the suitable margin of the relays TMS to provide proper coordination are stated as $TMS_{min} \leq t \leq TMS_{max}$. Where TMS_{min} is taken as 0.1 and $TMS_{max}$is taken as 1.2.

4 Operating Modes and Optimized Curves Setting

Adjustment of the relay settings to track the changes in the network topologies resulting from DG connection using optimization tool can be detected by an external control signal, this control signal may be one of the electrical variables (voltage- current- direction flow ….) or may be a switch status. A lot of calculations and well-defined control signals are required to implement an adaptive protection scheme that tracks the topology changes of the network with high penetrations level of DGs.

All the possibilities for IEC six-bus network in Fig. 1 could be summarized in the following points:

- There are six different locations for DG connection. so, for a defined DG size there are six-group optimized setting curves and six control signals would be needed.
- If the DG size is changed due to the switch of or switches on of some units, there are another six optimized setting curves are needed.
- If the network is expanding, and the bus numbers increase, the available possibilities of optimized setting curves will be increased.
- Due to the relatively long calculation time of the optimization algorithms, the adaptive relaying based on these algorithms should be offline. So, a lot of pre-calculated setting curves will be needed to cover all the available possibilities.
- Control signals should be defined accurately to enable the selection of the correct stored setting; it is a very difficult issue without an accurate communication channel.
- If the fault location, resistance, and type are involved, other relay settings should be available.

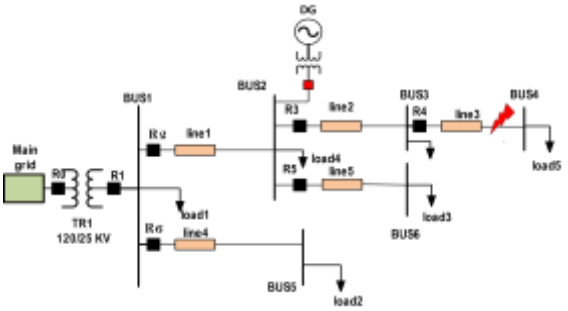

Fig. 2: IEC 6-bus radial network with DG connected at Bus2

It is very difficult to carry out all these calculations on -line, so the pre-calculated setting should be available. The settings of different cases (network without DG, with DG at different locations, different DG penetration levels) are calculated and stored in the memories of the OCRs, and an external signal for each case is defined and stored. The non-directional and directional OCR-optimized settings are tested and evaluated in the next section for different DG-connected scenarios.

5 Optimal Setting of Non-Directional OCR

Due to changes in the fault current magnitude measured at the relaying points if the DG connected at Bus 2 as in Fig. 2, the weights of the OF are changed, so, the new optimized values of TMSs (with both GA and GWO) are achieved as in Table 1. The new setting curves are achieved to track the changes in the network topology as in Fig.3. From Fig. 3, fault cases at the ends of line1, line 2, line 3, and line 4 respectively are carried out and the fault current magnitudes are recorded at the relaying points. The 4- bold vertical lines indicate the values of fault current magnitudes recorded at R_1, R_2, R_3, and R_4, and the red one indicates the reverse fault current magnitude sharing by DG for fault at Line 4 (recorded at R_2).

It is noticed that:

- The fault at line 3 could be detected and the coordination between R_4 and R_3 will be satisfied for fault cases at Line 3 (the intersection points between the fault current at line 3 and the setting curves of R_3 and R_4) the main and backup relay are forward of DG location.
- The fault case at Line 2 could be detected and the coordination margin (0.3sec) between R_3 and R_2 could not be achieved accurately due to the DG penetration of the fault current flows only at R_3.

- The fault at line 4 could be detected accurately by R_6, but the coordination with R_1 could not be achieved due to the fault infeed from DG (the margin between R_6 and R_1 is 0.7sec which is greater than 0.3). Moreover, false tripping due to reverse current does not occur in this case but if the DG size increases a false trip may be occurred (see the red vertical line resemble the reverse fault current infeed from DG and its intersection point with R_2 setting curve).

Table 1. The optimized values of TMS in the case of DG connection at Bus 2

Relay Number	TMS (GA)	TMS (GWO)
R_1	.2866	0.2876
R_2	0.3949	0.3962
R_3	0.2515	0.2523
R_4	0.1257	0.1261
R_5	0.1432	0.1551
R_6	0.1658	0.2092
Fitness value	6.40391	6.52662

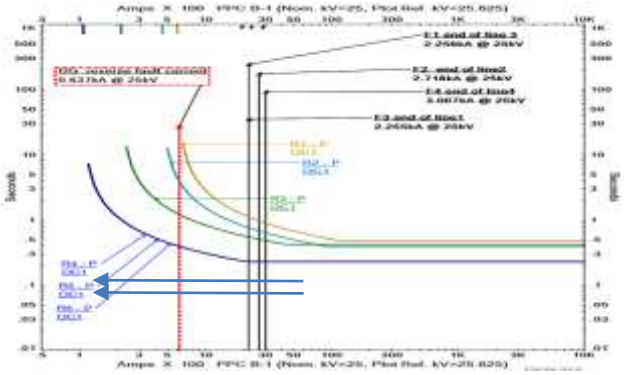

Fig. 3: Optimal relays setting curves for DG connection at Bus 2 scenario

Although the reverse current is not effective in this case, its influence is strong in the case of DG connection at Bus4 (see Fig. 4), and the selectivity of the relaying scheme is completely lost as in Fig. 5. For example, R_3, and R_4 lead the main and backup relays R_2 and R_1 for isolating the fault at Line 1 (see the vertical axis of F_3 at Line 1 and the vertical dash red line for the reverse fault current for F_3 at line 1).

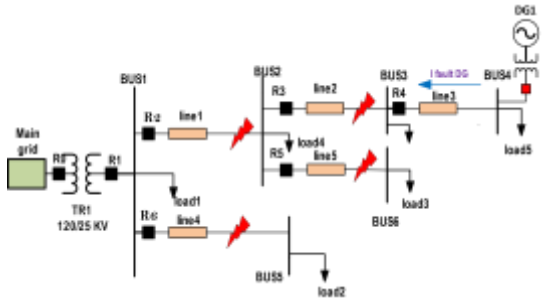

Fig. 4: IEC 6-bus radial network with DG connected at Bus4

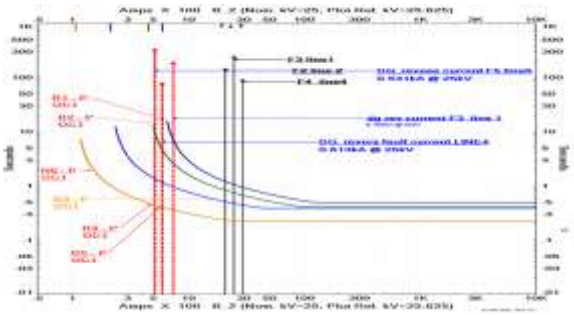

Fig. 5: Optimal relays setting curves for DG connection at Bus 4 scenario

Also, the relay R_4 leads R_3 for isolating F_2 at line 2. The same situation has been detected when the DG location is transferred to Bus 5 or Bus 6. From these results, it appears that: -

- The adaptive OCR scheme based on the optimal definition of the setting is valid only for a single branch radial feeder with small penetrated DGs connected as near as possible from the PCC of the utility.
- There is an urgent need for a directional OC relay to prevent a false trip due to reverse fault current that is recommended in many scientific literature, [19], [20], [21].

6 Optimal Setting of DOCR Scheme

For meshed systems, DOCRs become an attractive option due to the bi-directionality of fault currents. Recently, the directional discrimination principle is strongly recommended for DG-connected multi-infeed networks. As mentioned in, [10], [11], [12], [13], [14], for the IEC six bus network with different DG connected at different locations along the network, the authors have introduced an adaptive relaying scheme based on inserting an additional DOCR at the far end of each feeder-section to be concerned with the reverse current infeed. In this section, this scheme has been investigated and highlighted to show its effectiveness. As seen in Fig. 6, four DGs with different types are connected at

different buses of the IEC network. To provide a selective relaying scheme, 15 relays (R_1-R_{15}) are used to cover the new network topology and it should be coordinated as in Table 2. The coordination between relays must be updated to meet the expected changes in the fault current magnitude and direction based on DG location. The updating process comprises updating TMS values for the forward existing relays (R_1-R_6) and the new installation relays (R_7-R_{15}). The optimized values of TMS are achieved with GA and GWA. The constraints equations should be rearranged to guarantee the CIT between the main and backup relays according to the new relaying scheme design, the CTI value is taken as 0.3sec. The optimized TMS values of the DOC relaying scheme are achieved as in Table 3.

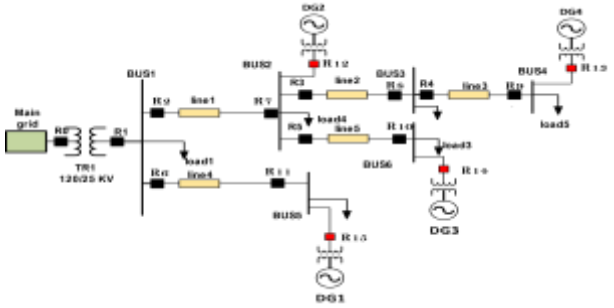

Fig. 6: IEC modified model with connecting 4-DGs and directional overcurrent relay.

Table 2. Primary and backup relays for different fault locations of the IEC network

Fault location	Line 1		Line 2		Line 3		Line 4		Line 5	
Primary relays	R_2	R_7	R_3	R_8	R_4	R_9	R_6	R_{11}	R_5	R_{10}
Backup relays	R_1 R_{11}	R_8 R_{10} R_{12}	R_2 R_{10} R_{12}	R_9	R_3 $R1_0$ R_{12}	R_{13}	R_1 R_7	R_{15}	R_2 R_8	R_{14}

6.1 The Fault at The End of Line 1

For a 3-phase short circuit at the end of Line 1 of the network in Fig. 6, from the utility side, R_2 and its backup group (R_1 and R_{11}) are concerned with isolating the line 1 fault from the BUS 1 side as a result to the forward fault current. From the far endpoint, R_7 and its backup group (R_8 - R_{10} - R_{12}) are concerned with isolating the line 1 fault from the BUS 2 side as a result of the reverse fault current.

Table 3. TMS values for stander and non-standard characteristics of IDMT using GA

Relay	TMS stander GA 1.1‹CMS‹ 20	TMS Non-stander GA 1.1‹CMS‹ 100	TMS stander GWO 1.1‹CMS‹ 20	TMS Nonstandard GWO 1.1‹CMS‹ 100
R_1	0.338	0.283	0.3401	0.2855
R_2	0.397	0.340	0.3988	0.4027
R_3	0.256	0.2358	0.2357	0.2795
R_4	0.132	0.1391	0.1328	0.1397
R_5	0.122	0.141	0.1431	0.1560
R_6	0.132	0.150	0.1932	0.1778
R_7	0.142	0.172	0.2107	0.1778
R_8	0.11	0.086	0.0888	0.0899
R_9	0.13	0.1739	0.1788	0.1777
R_{10}	0.069	0.0695	0.1055	0.1109
R_{11}	0.235	0.2226	0.2672	0.2247
R_{12}	0.186	0.1704	0.1767	0.1712
R_{13}	0.230	0.2437	0.2353	0.2051
R_{14}	0.116	0.1159	0.1468	0.1615
R_{15}	0.194	0.1936	0.2849	0.2491
T(s)	16.98	17.48	18.22	18.1735

Table 4. The operating time and fault current measured at the related relays for a fault at the end of line 1

Fault location	Fault current measurements (KA), and operating time t_{op} in (sec)						
	Main	Backup	Backup	Main	Backup	Backup	Backup
	R_2	R_1	R_{11}	R_7	R_8	R_{10}	R_{12}
Line 1	I_f=5.443 t_{op}=0.9	I_f=4.925 t_{op}=1.657	I_f=0.543 t_{op}=1.548	I_f=3.293 t_{op}=0.42	I_f=1.465 t_{op}=0.276	I_f=0.923 t_{op}=0.315	I_f=0.92 t_{op}=0.868

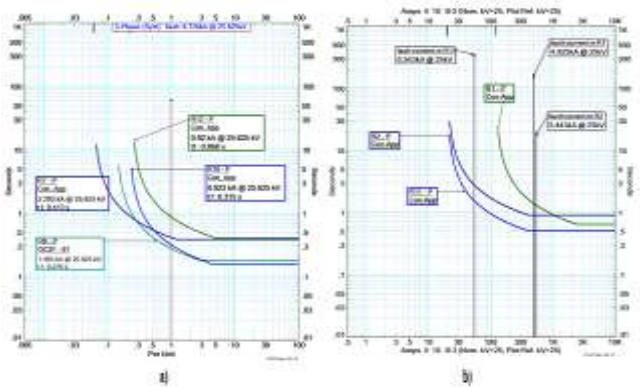

a. R2 and its backup relay characteristic curves.
b. R7 and its backup relay characteristic curves.

Fig. 7: Characteristics curves of the main and backup relays for Line 1 protection.

From Table 4, According to the relays operating time, the relays could be arranged according to the fast-tripping ones as R_8, R_{10}, R_7 , and finally R_2. As a result, unneeded tripping of DG3 and DG4 has occurred. According to the tripping sequence of

relays, the backup relays R_8, and R_{10} have tripped faster than the main one R_7 preventing the DG penetration in the reverse fault current, then the fault current measured at R_7 will be decreased and its tripping time will be increased, and the coordination problem could be aggravated. This problem is brightly indicated in the intersection of the main and backup relays setting curves at high fault current rating as in Fig. 7. Moreover, the problem of coordination between relays is strongly manifested when the same fault has occurred at the other end of Line 1 (near Bus 1), the fault current and its associated operating time for all relays are recorded in Table 5. Due to the fault location shifting from the location that is defined in the optimization process, the fault currents recorded at the relaying points are changed and its operation time is shifted on its setting curve as a result the pre-setting CIT could not be achieved for the forward and reverse direction relays.

Table 5. The operating time and fault current measured at the related relays for a fault at the beginning of line 1

Fault location	Fault current measurements (KA), and operating time t_{op} in (sec)						
	Main	Backup	Backup	Main	Backup	Backup	Backup
	R_2	R_1	R_{11}	R_7	R_8	R_{10}	R_{12}
Line 1	I_f=9.295 t_{op}=0.9	I_f=8.375 t_{op}=1.198	I_f=0.923 t_{op}=1.0	I_f=2.635 t_{op}=0.45	I_f=1.173 t_{op}=0.311	I_f=0.739 t_{op}=0.37	I_f=0.373 t_{op}=0.972

6.2 Fault at the End of Line 2

Although the false tripping due to the reverse current in the case study in the previous section, the optimized setting could keep the coordination between the main and backup relays for the same fault at the end of Line 2 as indicated in Table. 6. From Table 6 and the characteristic curves for each group that is indicated in Fig. 8, the main relays R_3, and R_8 have the lowest tripping time, and the CTI between the forward current relays and the reverse current relays has been achieved.

Table 6. The operating time and fault current measured at the related relays for a fault at the end of line 2

Fault location	Fault current measurements (KA), and operating time t_{op} in (sec)							
	Main	Backup	Backup	Backup	Backup	Main	Backup	Backup
	R_3	R_2	R_{10}	R_{12}	R_{14}	R_8	R_9	R_{13}
Line 1	I_f=4.683 t_{op}=0.6	I_f=3.51 t_{op}=0.9	I_f=0.595 t_{op}=1.3	I_f=0.594 t_{op}=1.08	I_f=0.595 t_{op}=0.972	I_f=1.648 t_{op}=0.25	I_f=1.648 t_{op}=0.552	I_f=1.648 t_{op}=0.879

6.3 Fault at the End of Line 3

For the 3-phase fault at the end of Line 3, it can be noticed that from Table 7, despite the coordination margin (0.3) could not be exactly achieved for the reverse current relays (R_9 and its backup relay), the forward current relays could maintain the CTI constraints. The fault could be successfully cleared from each side by R_4 and R_9 without any unwanted tripping, but the whole relaying scheme failed to be compatible with the CTI constraints.

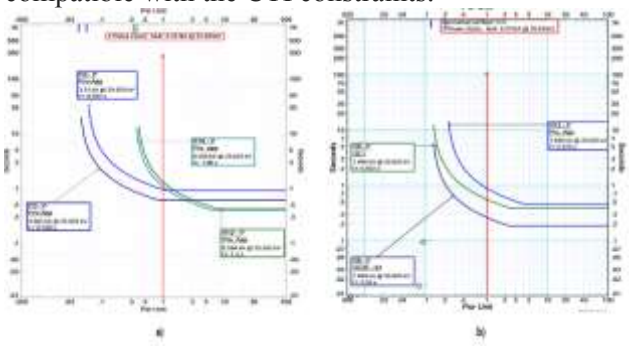

a) R3 and its backup relay characteristic curves.
b) R8 and its backup relay characteristic curves.

Fig. 8: Characteristics curves of the main and backup relays for Line 2 protection.

Table 7. The operating time and fault current measured at the related relays for a fault at the end of line 3

Fault location	Fault current measurements (KA), and operating time t_{op} in (sec)					
	Main	Backup	Backup	Backup	Main	Backup
	R_4	R_3	R_{10}	R_{12}	R_9	R_{13}
Line 1	I_f=3.456 t_{op}=0.315	I_f=3.456 t_{op}=0.63	I_f=0.439 t_{op}=1.5	I_f=0.438 t_{op}=1.88	I_f=1.884 t_{op}=0.519	I_f=1.884 t_{op}=0.808

6.4 Case 4 Fault at the End of Line 4

Referring to Table 8 which indicates the fault current measured at the related relays for a fault at the end of line 4, the coordination margin (0.3) could not be exactly achieved between the main forward relay R_6 and its backup relay R_7. On the other hand, the reverse current relays could be able to hold the CTI constraints.

Table 8. The operating time and fault current measured at the related relays for a fault at the end of line 4

Fault location	Fault current measurements (KA), and operating time t_{op} in (sec)				
	Main	Backup	Backup	Main	Backup
	R_6	R_1	R_7	R_{11}	R_{15}
Line 1	I_f=5.998 t_{op}=0.299	I_f=4.572 t_{op}=1.75	I_f=1.439 t_{op}=0.591	I_f=0.991 t_{op}=0.96	I_f=0.991 t_{op}=1.26

6.5 Fault at the End of Line 5

From Table 9, it can be noticed that R_5 and R_2 could keep the CTI constraints, but unfortunately, R_8 could not, so the coordination could not be achieved for all relays. In contrast, the selectivity between the reverse current relays has been completely lost since the backup relay has a lower operating time than the main one.

Table 9. The operating time and fault current measured at the related relays for a fault at the end of line 5

Fault location	Fault current measurements (KA), and operating time top in (sec)				
	Main	Backup	Backup	Main	Backup
	R5	R2	R8	R10	R14
Line 1	If=4.913 top=0.295	If=3.416 top=0.952	If=0.92 top=0.361	If=0.991 top=0.732	If=0.991 top=0.599

7 Results Discussions

Checking the constraints equations for each relay to test if the constraints are achieved or not for all fault locations. Faults [F_1-F_2-F_3-F_4-F_5] at feeder sections [Line 1-Line 2- Line 3- Line 4- Line 5] respectively.

It can be noticed that the opportunity of forward current relays to keep the preset CTI is larger than the reverse current relays (R_2, R_3, and R_4 are satisfied the coordination constraints), the other forward relays R_5 and R_6 are satisfied with the backup forward relays and are not satisfied for the reverse backup ones. The reverse current relays R_{11} and R_{12} completely satisfy the coordination constraints. R_7 and R_8 are the most violated relays to the constraints since their locations between the DGs connection points. The other relays satisfy the constraints sometimes and are violated at other times. It can be concluded that the reverse relays that are located between the DGs connection points are the ones violating coordination constraints. From equation 3, it can be noticed that each relay is coordinated multi-times with the main relay for different fault locations, this is the main cause of the confusion of DOCR scheme selectivity. So, this method could not provide a complete solution for selectivity problems if the DG location and size are demonstrated.

8 Increasing the Maximum Limit of CMS as a Solution of Mis-coordination

The researchers have introduced a non-standard characteristic of the DOCRs as a solution for mis-coordination associated with high fault current levels due to DG connection, [12], [22]. All the TMS optimization procedures are carried out with the new coordination constraints related to the overcurrent relay stander equation by considering the new limits of CMS values to be a fixed value (100 times the pickup current instead of 20 times in the standard equation) to enlarge the inverse region of the curve. This method has been tested for the network arrangement indicated in Fig. 9 considering new constraints related to the nonstandard curves.

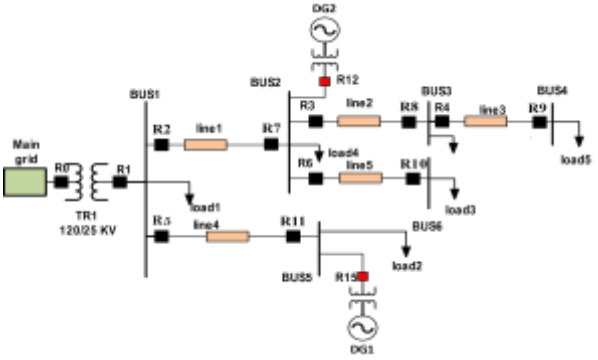

Fig. 9: IEC 6-bus network with two DGs at Bus 2 and Bus 5

From the optimized TMS values of the standard and non-standard equations of IDMT based relaying scheme, the characteristic curve of R_2 is plotted for each case as in Fig. 10. When a 3-phase short circuit occurred at the utility side end of Line 1, for conventional IDMT characteristic, the relay R_2 will operate within 0.807 sec, by the new non-standard curve the relay will trip the fault within 0.6358 sec. From the non-standard curve (dash line), the inverse region of the curve is stretching and hence the selectivity between the relays and the relay sensitivity are enhanced (the operating time of the relay is reduced from 0.807 to 0.6358). Although the relaying scheme based on non-standard characteristics has a good opportunity to maintain the coordination margin for high fault current, it could not resolve the coordination process accurately due to the relay participation in more than one coordination constraint not being resolved.

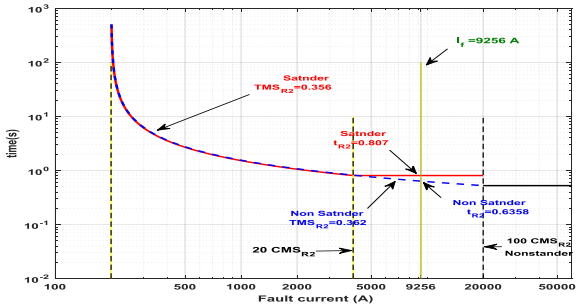

Fig. 10: R_2 characteristic curves for standard and non-standard IDMT equation.

9 Islanding Mode Operation

For any reason such as maintenance, or fault cases, the utility infeed will be lost, and the IEC micro-grid will be transferred into islanding mode and all its loads are fed from the DG only as shown in Fig. 11. Three phase short circuit at the ends of all the network lines are carried out, the fault current of the related relays for each fault location are recorded in the Table. 10. For this operation mode, the optimized values of TMS for standard curves of the IDMT relaying scheme are tabulated in Table. 11 With the obtained values of TMS, the relay characteristic curves are plotted, all the fault cases are tested, and relaying scheme performances are examined.

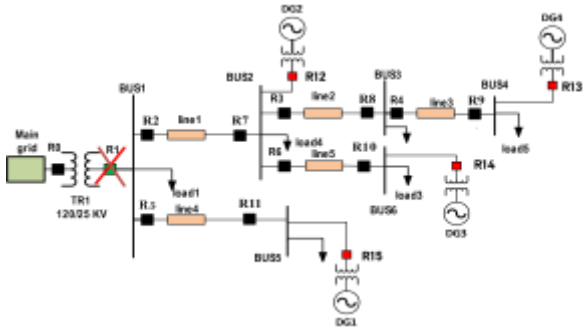

Fig. 11: IEC network without grid connection (islanding mode)

Table 10. Fault current measured at the relaying points for different fault locations of the network in Fig. 11

Fault location	Fault current measurements (KA)													
	R_2	R_3	R_4	R_5	R_6	R_7	R_8	R_9	R_{10}	R_{11}	R_{12}	R_{13}	R_{14}	R_{15}
Line 1	0.923					2.635	1.173		0.739	0.923	0.373			0.923
Line 2	0.864	2.693					1.465	1.465	0.923		0.92			
Line 3		2.239	2.239					1.648				1.648		
Line 4				2.635		2.635				0.923				0.923
Line 5	0.864				3.236		1.465		0.923		0.92		0.923	

Table 11. TMS Values for isolating mode

Relay	TMS (stander curve)
R_2	0.181
R_3	0.21
R_4	0.105
R_5	0.105
R_6	0.112
R_7	0.209
R_8	0.086
R_9	0.173
R_{10}	0.069
R_{11}	0.247
R_{12}	0.177
R_{13}	0.193
R_{14}	0.115
R_{15}	0.264
T(s)	19.18

9.1 Fault at The Utility End of Line 1

For a 3-phase short circuit at the utility end of Line 1in Fig. 11, the measured fault current at the related relays and its operating time is tabulated in Table 12. It can be noticed that the forward current relay R_2 and its backup one R_{11} failed to keep the presetting value of CTI (CTI value is 0.294 sec). In contrast, the coordination between the reverse fault current relays (R_7 and its backup relays R_8, and R_{10}) has been completely lost, since R_8 and R_{10} provide an operating time less than that of the main relay R_7, and the unneeded isolation of DG3 and DG4 has resulted. The coordination of directional over the current relay based on GA failed in this case.

Table 12. The operating time and fault current measured at the related relays for a fault at the utility end of line 1

Fault location	Fault current measurements (KA), and operating time t_{op} in (sec)					
	Main	Backup	Main	Backup	Backup	Backup
	R_2	R_{11}	R_7	R_8	R_{10}	R_{12}
Line 1	I_f=0.923 t_{op}=0.816	I_f=0.923 t_{op}=1.11	I_f=2.635 t_{op}=0.553	I_f=1.173 t_{op}=0.334	I_f=0.739 t_{op}=0.356	I_f=0.373 t_{op}=2.0

9.2 Fault at Utility-End of Line 2

As in Table 13, for the fault case at the utility end of Line 2, the coordination between the forward current relays R_3 and R_2, and R_{12} has been accurately achieved. However, the coordination with R_{10} failed to be obtained as a result undesired tripping of DG3 has resulted. Also, the reverse current main relay R_8 and its backup relays R_9 could keep the CTI constraints accurately, see Fig. 12.

Table 13. The operating time and fault current measured at the related relays for a fault at the utility end of line 2.

Fault location	Fault current measurements (KA), and operating time t_{op} in (sec)					
	Main	Backup	Backup	Backup	Main	Backup
	R_3	R_2	R_{10}	R_{12}	R_8	R_9
Line 1	I_f=2.693 t_{op}=0.551	I_f=0.864 t_{op}=0.853	I_f=0.923 t_{op}=0.311	I_f=0.92 t_{op}=0.853	I_f=1.465 t_{op}=0.296	I_f=1.465 t_{op}=0.596

9.3 Fault at the Utility End of Line 4

For the fault at line 4, the coordination is completely lost between the reverse current relays R_{11} and R_{15}, and nearly maintain with CTI value (0.275) for the forward fault relays R_5 and R_7, see Fig. 13 in which the intersection between the curves of R_{11} and R_{15} is remarkable from the low fault current level region. In this fault case, the directional over current relay with optimized TMS failed to provide selective protection.

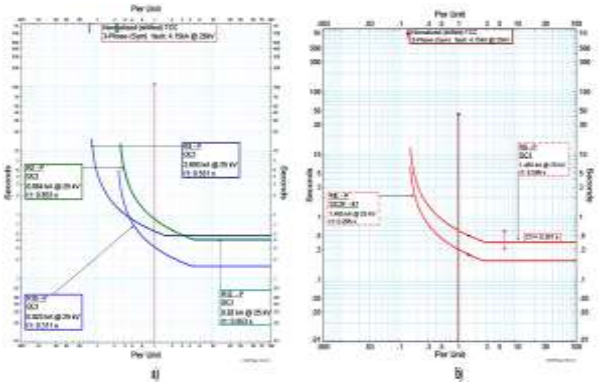

a) R_3 and its backup relay characteristic curves.
b) R_8 and its backup relay characteristic curves.

Fig. 12: Characteristics curves of the main and backup relays for Line 2 protection

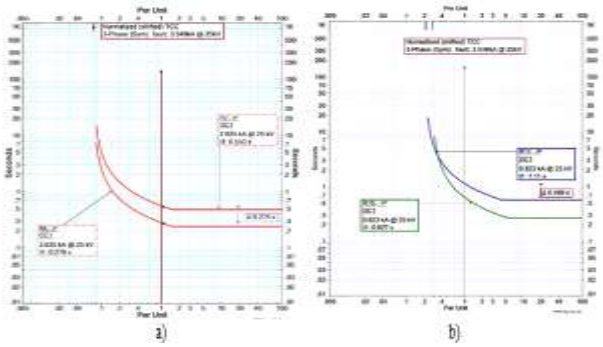

a) R5 and its backup relay characteristic curves.
b) R_{11} and its backup relay characteristic curves.

Fig. 13: Characteristics curves of the main and backup relays for Line 4 protection

10 Conclusion

The optimized setting of the DOCR scheme has been recently introduced as a solution to the mis-coordination problem of multi-infeed DG-grid connected. Different optimization tools such as GA, PSO, WCA…etc. are competed to provide the lowest calculation time to provide an optimized DOCR-scheme setting. In this paper, the performance of this scheme for different fault locations and different operating modes for multi-in-feed DG-connected grids is evaluated. Most of the works of literature are concerned with only one case with a fixed size, and location of the DG units to provide an efficient coordination, and the primary and backup relay pairs are only demonstrated. In this paper, all the backup relays that the reverse fault current passes through are concerned to test the relaying scheme selectivity. The results showed that the CTI value that has been constrained in the training process (CTI = 0.3) may not be obtained elsewhere since the relay is forced to be coordinated with different relays and keeps the CTI constraints. Actually, each relay is required to coordinate with more than one relay and maintain the CTI constraints (each relay is required to be trained in multi-constraints equations in GA calculations), it is a difficult issue to guarantee a selective relaying scheme. Moreover, the results based on the optimization tools are restricted by the input data that are being trained on, if any deviation occurs on this data, the output variables of the optimization tools may provide unexpected or completely false results. Due to unequal fault current detected at the two line terminals, and mismatched curves of the main relays, the fault is not isolated from the two ends at the same time. One end trip first and the other end will follow it, so there is a need for a communication network. However, the optimized setting of the DOCR scheme could reduce the number of relays that provides false tripping, there are still unwanted tripping sections due to mis-coordination resulting from the architecture of the OF, in which the relay is sharing multi-constraint equations. Finally, this method is not a sufficient solution for selectivity problems as demonstrated in the literature, and the resetting of the traditional equation curve of OCR should be reconsidered. Also, DG location, size, types, obedience to grid codes, and its local control and protection system should be involved in any future study. However, limits DG output current according to DG terminal voltage, Optimal DG size and location, and another innovative technical solutions are introduced to solve this problem, it is still needed an adaptive smart protection system independent of traditional

OCR setting curves. In our future work, a wavelet scattering network-based machine learning is used to implement a smart protection system for a multi-infeed DG-connected grid.

References:

[1] D. R. Bhise, R. S. Kankale and S. Jadhao, "Impact of distributed generation on protection of power system, " *International Conference on Innovative Mechanisms for Industry Applications* (ICIMIA), 2017, pp. 399-405.

[2] M. Meskin, A. Domijan, and I. Grinberg, ."Impact of distributed generation on the protection systems of distribution networks: Analysis and remedies – review paper, " *IET Generation, Transmission and Distribution*, Vol. 14, No. 24, 2020, pp. 5816–5822.

[3] N. M. Mansour, E. S. Oda, E. E. Omran and A. A. Abdelsalam, ."An Analytical Investigation Review of DG Impacts on the Relaying Performance in Distrbution Networks", *22nd International Middle East Power Systems Conference (MEPCON),* No. 22, 2021, pp. 137-143.

[4] P. P. Barker and R. W. De Mello, ."Determining the impact of distributed generation on power systems: Part 1 - Radial distribution systems", *Proceedings of the IEEE Power Engineering Society Transmission and Distribution Conference*, Vol. 3, No. c, 2000, pp. 1645–1656.

[5] A. D. Udgave and H. T. Jadhav, "A review on Distribution Network protection with penetration of Distributed Generation, " *2015 IEEE 9th International Conference on Intelligent Systems and Control (ISCO)*, Coimbatore, India, No. 9 2015, pp. 1-4.

[6] R. Ogden and J. Yang, ."Impacts of distributed generation on low-voltage distribution network protection, " *Proceedings of the Universities Power Engineering Conference*, vol. 2015-Novem, pp. 4–9.

[7] M. Yousaf and T. Mahmood, ."Protection coordination for a distribution system in the presence of distributed generation", *Turkish Journal of Electrical Engineering and Computer Sciences*, Vol. 25, No. 1, 20172017, pp. 408–421.

[8] M. Usama et al., ."A Comprehensive Review on Protection Strategies to Mitigate the Impact of Renewable Energy Sources on Interconnected Distribution Networks", *IEEE Access*, Vol. 9, 2021, pp. 35740-35765.

[9] V. Telukunta, J. Pradhan, A. Agrawal, M. Singh, and S. G. Srivani, ``Protection challenges under bulk penetration of renewable energy resources in power systems: A review," CSEE J. Power Energy Syst., Vol. 3, no. 4, 2017, pp. 365-379, Dec. 2017.

[10] Ke Xu , Yuan Liao."Intelligent Method for Online Adaptive Optimum Coordination of Overcurrent Relays."2018 *Clemson University Power System Conference (PSC),* 2018, pp.1-5, doi: 10.1109/ PSC.2018.8664055.

[11] N. E. Naily, S. M. Saad, M. M. El Misslati and F. A. Mohamed, "Optimal Protection Coordination for IEC Microgrid Benchmark Using Water Cycle Algorithm," 2019 *10th International Renewable Energy Congress (IREC)*, 2019, pp. 1-6, doi: 10.1109/IREC.2019.8754511.

[12] Hatata, Ahmed & Kaddah, Sahar & Abdraboh, H & Frahat, M. (2014). "Optimal Directional Overcurrent Relay Coordination Using Artificial Immune Algorithm". Vol. 39, 2014, pp. 9-18. 10.21608/bfemu.2020.102738.

[13] F. Alasali, E. Zarour, W. Holderbaum and K. N. Nusair, "Highly Fast Innovative Overcurrent Protection Scheme for Microgrid Using Metaheuristic Optimization Algorithms and Nonstandard Tripping Characteristics", in *IEEE Access*, Vol. 10, 2022, pp. 42208-42231, doi: 10.1109/ACCESS.2022.3168158.

[14] Sergio D. Saldarriaga-Zuluaga, Jesús M. López-Lezama, Nicolás Muñoz-Galeano, "Optimal coordination of over-current relays in microgrids considering multiple characteristic curves", *Alexandria Engineering Journal*, Vol. 60, Issue 2, 2021, pp. 2093-2113.

[15] M.-T. Yang and A. Liu, "Applying hybrid Pso to Optimize Directional Overcurrent relay coordination in Variable network topologies," *Journal of Applied Mathematic*s, vol. 2013, pp. 1–9, 2013.

[16] D. Uthitsunthorn, P. Pao-La-Or, and T. Kulworawanichpong, "Optimal overcurrent relay coordination using artificial bees colony algorithm," *The 8th Electrical Engineering/ Electronics, Computer, Telecommunications and Information Technology (ECTI) Association of Thailand* - Conference 2011, 2011.

[17] V. Rashtchi, J. Gholinezhad, and P. Farhang, "Optimal coordination of OVERCURRENT Relays using honey Bee algorithm," *International Congress on Ultra-Modern*

Telecommunications and Control Systems, 2010.

[18] Kar, S. A comprehensive protection scheme for micro-grid using fuzzy rule base approach. *Energy Syst 8*, pp. 449–464, (2017). https://doi.org/10.1007/s12667-016-0204-x.

[19] J. S. Farkhani, M. Zareein, H. Soroushmehr and H. M. SIEEE, "Coordination of Directional Overcurrent Protection Relay for Distribution Network With Embedded DG," *2019 5th Conference on Knowledge Based Engineering and Innovation (KBEI)*, 2019, pp. 281-286, doi: 10.1109/KBEI.2019.8735025.

[20] D. K. Jain, P. Gupta and M. Singh, "Overcurrent protection of distribution network with distributed generation," *2015 IEEE Innovative Smart Grid Technologies - Asia (ISGT ASIA)*, 2015, pp. 1-6, doi: 10.1109/ISGT-Asia.2015.7387143.

[21] N. K. Choudhary, S. R. Mohanty and R. K. Singh, "Protection coordination of over current relays in distribution system with DG and superconducting fault current limiter," *2014 Eighteenth National Power Systems Conference (NPSC)*, 2014, pp. 1-5, doi: 10.1109/NPSC.2014.7103818.

[22] Abdallah Reda, Amal F. Abdelgawad, Mohamed Ibrahim,"Effect of non standard characteristics of overcurrent relay on protection coordination and maximizing overcurrent protection level in distribution network", *Alexandria Engineering Journal*, Vol. 61, 2022, pp. 6851-6867.

Appendix

The details of the studied system are given as follows:

Utility: rated short-circuit MVA=1000, f=60 Hz, rated kV=120, Vbase =120kV.

Distributed Generations (DGs):

- DG1, DG2: Synchronous generator with rated MVA=9, *f*=60Hz, rated kV=2.4, Inertia constant H=1.07 s, friction factor F=0.1 pu, Rs=0.0036 pu, X_d=1.56 pu, $X_d^{\backslash\backslash}$=0.296 pu, $X_d^{\backslash}$ =0.177 pu, X_q=1.06 pu, $X_q^{\backslash\backslash}$=0.177 pu, Xl=0.052 pu, $T_d^{\backslash}$ =3.7 s, $T_d^{\backslash\backslash}$=0.05 s, Tqo =0.05 s.
- DG3: Wind farm consisting of three 2 MVA wind turbines (6 MW, pf=0.9), *f*=60 Hz, rated kV = 575 V, inertia constant H = 0.62 s, friction factor F = 0.1 pu, Rs = 0.006 pu, X_d = 1.305 pu, $X_d^{\backslash}$= 0.296 pu, $X_d^{\backslash\backslash}$= 0.252 pu, X_q = 0.474 pu, $X_q^{\backslash}$= 0.243 pu, X_l = 0.18 pu, $T_{do}^{\backslash}$ = 4.49 s, $T_{do}^{\backslash\backslash}$ = 0.0681 s, $T_q^{\backslash\backslash}$ = 0.0513 s. 575 V, 60 Hz. (Type-4 detailed model in MATLAB/SIMULINK).
- DG4: DFIG based wind farm consisting of six 1.5 MVA wind turbines (9 MVA, pf = 0.9), f = 60 Hz, rated kV = 575 V, Inertia constant H = 0.685 s, frictionfactor F = 0.01 pu, R_s = 0.023 pu, L_{ls} = 0.18 pu, R_r = 0.016 pu, L_{lr} = 0.16 pu, L_m = 2.9 pu.

Transformers (TRs):

- TR_1: Rated MVA = 50, *f* = 60 Hz, rated kV = 120 kV/ 25 kV, V_{base} = 25 kV, R_1 = 0.00375 pu, X_1 = 0.1 pu, R_m = 500 pu, X_m = 500 pu.
- TR_2 and TR_4: Rated MVA = 12, *f* = 60 Hz, rated kV = 2.4kV/ 25 kV, V_{base}= 25 kV, R_1 = 0.00375 pu, X_1 = 0.1 pu, R_m = 500 pu, X_m = 500 pu.
- TR_3 and TR_5: Rated MVA = 10, *f* = 60 Hz, rated kV = 575 V/ 25 kV, V_{base} = 25 kV, R_1 = 0.00375 pu, X_1 = 0.1 pu, R_m = 500 pu, X_m = 500 pu

Contribution of Individual Authors to the Creation of a Scientific Article (Ghostwriting Policy)

- Emad Eldeen Omran, carried out the simulation and the optimization Algorithm using Matalb and ETAP software backags.
- Naema M. Mansour has organized, analyzed and formulated the results.
- Abdelazeem A. Abdelsalam and Eyad S. Oda have supervised the formulation of the problem and the final review of the research and evaluating the results.

Sources of Funding for Research Presented in a Scientific Article or Scientific Article Itself

No funding was recived for conducting this study.

Conflict of Interest

The auters have no conflict of interst to declare.